Digitally Beamformed Multibeam Phased Array Antennas for Future Communication Satellites

A.S. Daryoush
Department of ECE, Drexel University, Philadelphia, PA 19104, USA
Daryoush@ece.drexel.edu

***Abstract* – Future generation of communication satellites are based on multi-beam phased array antennas, where beamforming and scanning are all fully implemented in digital domain as opposed to the commonly considered analog domains. The challenges of realizing a digitally beamformed multi-beam phased array antennas are many when communications are intended for applications beyond Q-band communication satellites, where RF down-conversion, phase control and timing synchronization, analog-to-digital conversion, and ultra high-speed data links are the important functions before the digital signal processing function could be implemented. The down-conversion and phase shifting could be combined using ILPLL systems that are implemented in both electrical and optical domains. Design of a novel all-optical ADC using spectral technique is presented, where sampling speeds as high as 50GS/s with a minimum 6 bits of resolution is attainable with maximum power consumption of 4W.**

***Index Terms* –** *communication satellites, multibeam phased array antenna, RF down conversion, ILPLL, beam scanning, optical ADC, optical data network*

I. Introduction

The next generation of global wireless communications utilizes communication satellites to provide interconnectivity anywhere in the world, especially in areas with poor telecommunications infrastructures or when rapid establishment of secure communications is demanded. Key requirement is to provide broadband access for video, data, and voice communications using carriers at millimeter wave (MMW) frequencies. Multibeam phased array antennas using digital beamforming network (DFBN) architectures [1] are implemented with multibeam algorithms using parallel processors based on high-speed digital data links. This architecture has greatest flexibility for reconfiguration in software defined radios. Figure 1 depicts a conceptual block diagram of a DBFN. The system architecture is based on the phased array antennas with sub-array level front end electronics, which provides down-conversion to IF/baseband signal from RF frequencies of Q band. It is followed by timing synchronization function to assure appropriate true delays for the beam scanned in various directions using optical techniques, analog-to-digital converter with n-bits of resolution, and fiber-optic data links providing connections from front end electronics to back-end signal processor to achieve various signal processing functions, such as digital beamforming. This approach requires ultra high-speed analog-to-digital converter. The goal of this paper is to discuss important RF and digital building blocks studied as part of digital beamforming networks with special emphasis on a newly developed all-optical analog-to-digital converters (AOADC) with operating speeds approaching 50 GS/s with resolution beyond 5 bits.

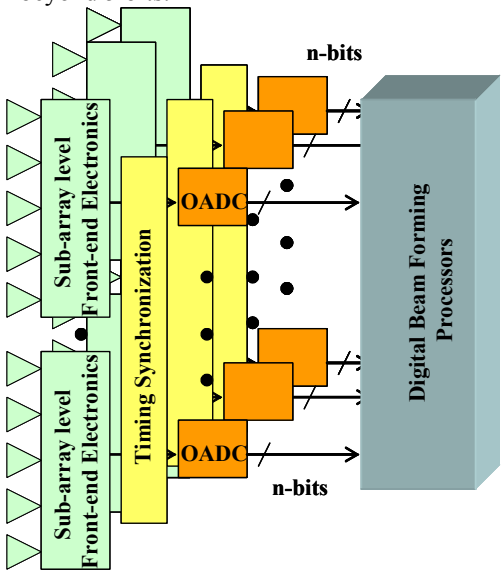

Fig. 1. Block diagram of antenna front-end for the digitally beamformed phased array antennas for communications.

II. RF Front End Manifold

Frequency Stabilization and Down-Conversion: To achieve a very low timing jitters digital bit streams, the overall phase noise of down converted signal has to be low; hence implementation of low phase noise MMW local oscillators and their efficient phase shifting has been of concern [2]. The concept of phase and frequency stabilized cascaded oscillators have been demonstrated using injection-locked phase lock loops (ILPLL), where excellent performance were reported in terms of phase noise and coherency of distributed locked oscillators [3]. The observed performance compares well with the frequency multiplier approach without suffering from higher power consumption[4]. Moreover, the concept of self-oscillating mixer has been combined with the ILPLL to attain efficient combined oscillator stabilization and frequency translation with good conversion gain [5]. Figure 2 depicts the measured frequency down-conversion of FM modulated RF at Ka-Band frequencies of 33 GHz to IF frequency of 9GHz using a stabilized 24 GHz local oscillator. The ILPLL has been employed for phase control of over 360^{o} in cascaded oscillators [3], and this phase shift can also be transferred to the down-converted IF or up-converted RF signals in the subarray [2].

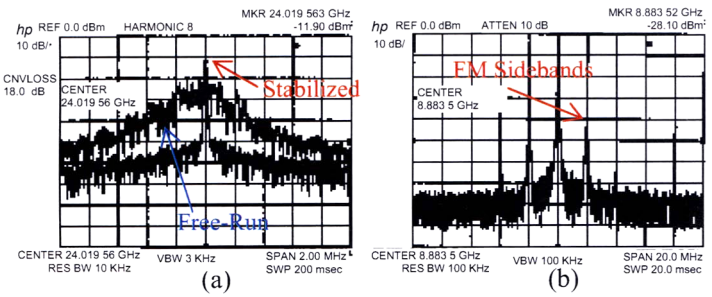

Fig. 2. Performance of a 24 GHz SOM. a) Spectra of the ILPLL stabilized and free-running 24GHz oscillators; b) down-conversion of the FM side-bands from RF (33GHz) to 9 GHz IF in the SOM [4].

True-Time Delay: Another important front end processing block is timing synchronization of each subarray. The fiber optic based switched delay lines are identified for achieving the required quantized phase profile as beam is scanned in various directions [6]. Figure 3 depicts comparison of two concepts of T/R- and CPU- level data mixing for RF of 31-34GHz. In Fig. 3a a greater performance is observed over the results of Fig. 3b since the scanned beam is realized using a continuous phase shift of LO 24GHz, while a lower resolution time delay of 30ps is employed with IF of 9GHz. Appreciable amplitude and side-lobe degradation penalties are observed even for a higher resolution time delay of 10ps in the RF path.

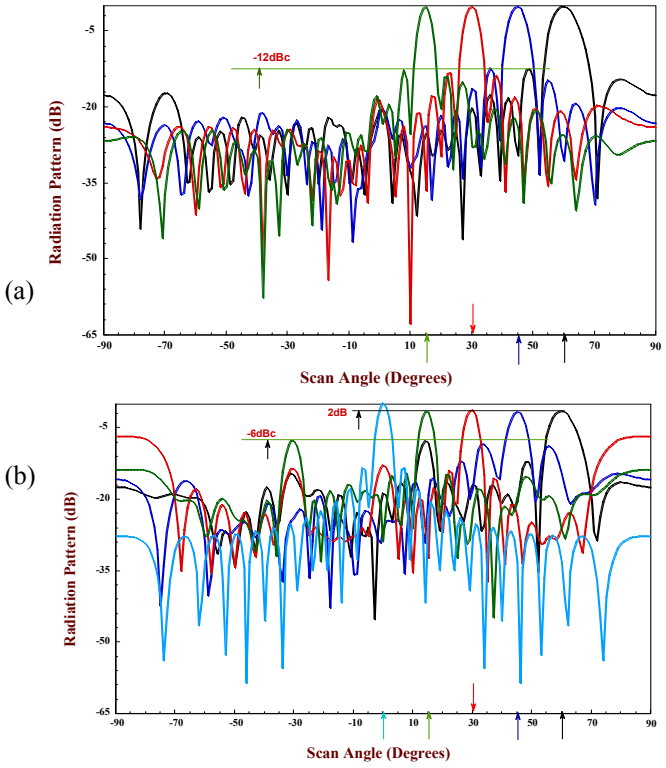

Fig. 3. Comparison of multiple co-phasal beams formed along scan angles of 0, 15, 30, 45, and 60 degrees for 13 linear array elements. a) A high-resolution time delay of 10ps for the RF signal; b) a lower resolution of 30ps for IF signal as a continuous phase shift of LO is maintained [7].

III. GS/S Digital Manifold

Analog-to-digital Converter (ADC): The properly down-converted and timing synchronized signals are digitized using high resolution ADC and employed for multi-beam digital beamforming process. For example for a 10% bandwidth at V-band, a Nyquist sample rate as high as 10 GS/s is required with a resolution of ENOB= 8, when a 50 dB SINAD is maintained. Since the state-of-the-art electronic ADC could provide a few bits of resolution for speeds of 10 GS/s and suffer from excessive power consumption [8], alternative techniques using optical ADC has been explored [9].

Optical ADCs are inherently superior in sampling speed to their electronic counterparts due one to two orders of magnitude smaller timing jitters of mode-locked lasers. Besides the obvious advantage of high sampling speeds, optical ADCs offer decoupling of the optical post sampled signal from the electrical signal being sampled. Moreover, digitized optical signals are easy to distribute and manage and are compatible with all optical signal processing functions. A number of optical ADC schemes have been proposed [10, 11]; however due to poor optical quantization and feasibility, all-optical ADCs have not been implemented in any practical applications. As a compromise, hybrid optical ADC structures have been proposed by incorporating optical sampling and electronic quantization. As an example, Bhushan, et al. demonstrated a record high speed ADC at 130 GS/s and 7.2 bits (effective) by time stretching of RF signal in optical domain [12]. Although this performance is only applicable for pulsed signals, it highlighted the high-speed capabilities of optical A/D conversion; however, hybrid ADCs suffers from mismatch of channels and high power consumption.

A novel all-optical ADC (AOADC) is presented in detail in section III, where optical sampling of IF signals and quantization are performed in the spatial domain. The option of realizing a spatial domain quantizer significantly reduces amplitude errors over amplitude quantizers that are employed by current ADCs.

Data Distribution Link: DBFN could be implemented using either DFT or FFT. The DFT is based on complex multiplier followed by summation, whereas FFT algorithm is based on radix 2 butterfly. The DFT is less attractive than FFT, when the number of beams is larger than $\log_2 N$ for an N receivers. The number of Butterflies required for a fully implemented FFT array is $(N/2)*(\log_2 N)$. When a single butterfly requires 22 gates, for 128 receivers with time-domain single-precision complex inputs (i.e., 1 bit/real and 1 bit/imaginary) and double-precision complex outputs (i.e., 2 bits/real and 2 bits/imaginary) a total of 9,856 gates are required. The complexity of the Butterfly grows very approximately O(q) for an implementation using only adders and shifters and $O(q^2)$ for a design using the faster array multipliers for q-bit precision data. Figure 4 depicts block diagram of a digital fiber-optic link to share data from ADC to the DFT/FFT based multibeam signal processor. The encoder/decoder circuits are designed for better edge detection using light weight protocols to reduce latency and maximize throughput. Both 8B10B and S-20 are attractive and currently being pursued. In the case of 8B10B, the 8 bit of parallel lines is

now converted to 10 bits requiring 100Gb/s digital fiber optic link. Performing a 10 bit serializer requires clock signal at 100GHz, where the cascaded ILPLL could be employed to provide stable oscillation up to 100GHz [4]. More recently, opto-electronic oscillator concepts based on hollow-core photonic crystal fibers (HC-PCF) has been employed to demonstrated passive temperature stabilization technique for opto-electronic oscillators [13].

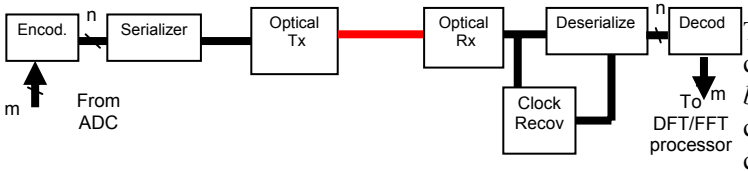

Fig. 4. Functional diagram of the fiber optic network.

The basic function units in serializer/deserializer circuits are: a) inverter, b) D-flipflop, and c) 2:1 multiplexer. The deserializer is essentially a shift register composed of 8 D-flipflops and serializer is a shift register with shift/load control. In absence of 100Gb/s foundry services, 10Gb/s serializer/deserializer circuits are designed and simulated based on typical AlGaAs ECL and SiGe NMOS foundry values respectively. Since CMOS circuits suffer from low speed caused by slow response PMOS transistor, the depletion loaded NMOS inverters are considered. Rise times of 19ps and 15ps are achieved for the inverter circuits using SiGe and AlGaAs HBT respectively with a resulting power consumption of 1.88W and 1.82W for serializer/deserializer circuits respectively.

IV. All Optical ADC (AOADC)

The system diagram of a general spatial sampling ADC is depicted in Figure 5. Mode-locked laser pulses are sent to an electro-optic (E-O) deflector, which deflects the optical beam to an angle θ that is proportional to the magnitude of the signal to be digitized. The optical pulses sample the signal at precise time intervals, and the position at an image plane where a pulse appears represents the amplitude it experienced at its sampling instance. Thus the spatial sampler converts the analog signal into time-discrete angular displacement. At the image plane an optical collector array performs as the spatial quantizer/coder by converting the applied RF signal to deflected angles.

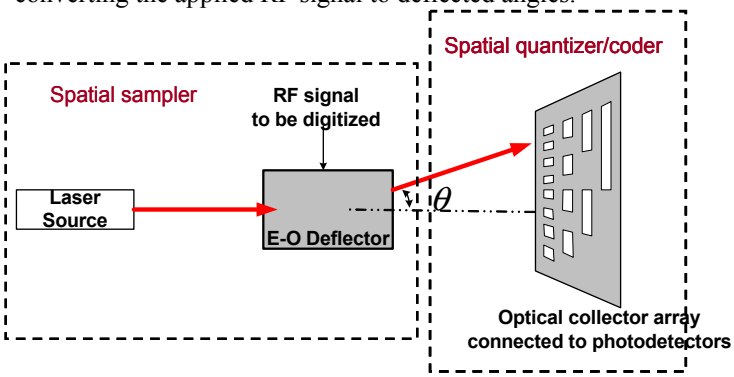

Fig. 5. Conceptual system diagram of AOADC with a E-O deflector as spatial sampling and optical collector as spatial quantizer.

By quantizing in the spatial domain, the problems associated with previous optical ADCs, such as sensitivity to the intensity of the optical pulses, are eliminated. The resolution of the AOADC is mainly determined by the angular resolution of the optical spatial sampler. The total number of resolvable image spots of the deflector is,

$$N = \frac{full\_scale\ angular\ swing}{angular\ resolution}.$$

Therefore the full span can be divided into N segments, corresponding to N quantization levels. So we can obtain $b=log_2(N)$ bits by using b columns of collector apertures. The collected optical power is essentially an optical binary signal that can be connected using optical fibers to the processor end, regenerated and further processed. Figure 6 shows the dispersion surfaces for homogenous waves inside the optical waveguide and the superstarte with a higher index of refraction than the optical waveguide (i.e., $n_s>n_{eff}$). As the superstarte index of refraction is modified from, n_1 to n_{eff} due to the applied RF voltage, a deflection in leaky wave angle is observed in the superstrate, which then results in change in the output angle. The swing in the output angle vs. applied RF electric field demonstrates a linear dependence on the applied RF voltage. A higher angular swing is observed for E-O polymer than $LiNbO_3$.

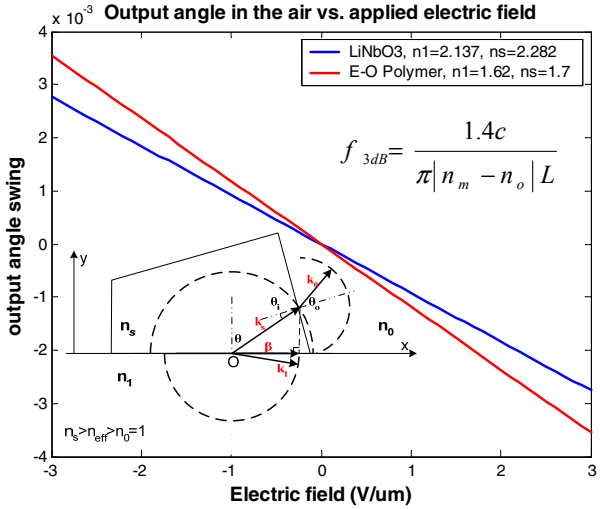

Fig. 6. Output angle swing (in radians) of the leaky wave EO deflectors in air as a function of the applied RF electric field. EO deflector's 3dB bandwidth is limited by deflector length L and velocity mismatch.

Note the angular swing at voltage of 20V is 2.8 mrad for $LiNbO_3$ superstrates, when the edge of the superstrate is at 60° with respect to the leaky waves. An RF signal with amplitude of 20V varies between +20 V and –20 V, therefore the total angular swing of the full scale is 5.6 mrad. A typical value of waveguide attenuation of 0.1 Np/cm is chosen to be add on top of the leakage loss of 0.19 Np/cm. Therefore after 3 cm, only 16% of the total launched power remains in the waveguide. While the total leaked optical power is 60% of the launched power. The combined attenuation of 0.29 Np/cm leads to an

angular resolution of 0.125 mrad. Therefore the total number of resolvable image line is 45. In principle, it is sufficient to implement a 6-bit AOADC using binary code with speeds of over 50GSPS with power dissipation of 4W. The quantized performance for a 5bit resolution AOADC is rendered in Figure 7, where an integral and differential nonlinearity of less than ½ LSB is observed.

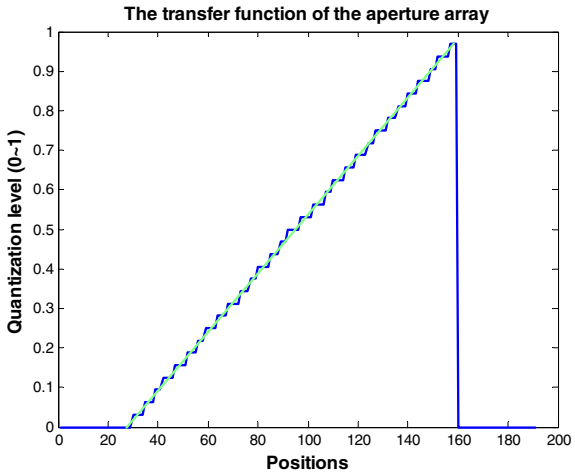

Fig. 7. Quantized output of 5 bit AOADC with excellent nonlinearity.

The high-sampling rate of the spatial sampling AOADC is guaranteed by using advanced mode locked lasers and photodetectors with bandwidth of order 100 GHz. But the more important instantaneous RF bandwidth is determined by the modulation bandwidth of the E-O deflector component. High-speed E-O polymer modulators operating up to 110GHz have been demonstrated [14]. E-O polymers also feature superior E-O coefficients of more than 70 pm/V, and current reports have shown E-O coefficient as high as 126 pm/V[15, 16], greatly enhancing the bandwidth-length product of E-O modulators.

V. Conclusion

A number of challenges associated with design of digital beam forming network are discussed for multibeam millimeter wave phased arrays antennas. The RF manifold is based on the frequency down-conversion to IF bandwidth using frequency stabilized SOM and optical timing synchronization using phase shifting of LO and true time delay for data signal. The emphasis is made on design of a novel all-optical ADC using polymer based E-O deflector with as many as 7 bits of resolution and sampling speed of over 50GS/s without consuming more than 4W of power. As the technological base required for each system function, the full integration of various sub-system components with the signal processor is the next challenge.

References

[1] A.S. Daryoush, H. Ogawa, A. Paolella, D. Zimmerman, "Beamforming Techniques for Active Phased Array Antenna-band Communication Satellites," *Workshop WFFT in 1999 IEEE International Microwave Symposium*, Anaheim, CA June 1999.

[2] X. Zhou, X. Zhang, and A.S. Daryoush, "A New Approach for a Phase Controlled Self-Oscillating Mixer," *IEEE Trans. Microwave Theory and Techniques*, Vo. 45, no. 2, pp. 196-204 , Feb. 1997.

[3] X. Zhang and A.S. Daryoush, "Full 360^{o} Phase Shifting of Injection Locked Oscillators," *IEEE Microwave and Guided Wave Letters,* vol. 3, no. 1, pp. 14-16, 1993.

[4] A. S. Daryoush, "Phase noise degradation in nonlinear fiber optic links distribution networks for communication satellites," Chapter 6 of Part 4 of *Microwave Photonics from Components to Applications and Systems*, edited by Anne Vilcot, Béatrice Cabon, Jean Chazelas, Ed, Kluwer Academic Publishers, May 2003.

[5] M. R. Tofighi and A. S. Daryoush, "A 2.5 GHz InGaP/GaAs Differential Cross-Coupled Self-Oscillating Mixer (SOM) IC," *IEEE Microwave and Wireless Component Lett.,* vol. 15, No. 4. pp. 211-213, April 2005.

[6] Y. Liu and J. P. Yao "Wideband true time-delay beamformer employing a tunable chirped fiber grating prism," App. Opt., vol. 42, no. 13, pp. 2273-2277, May 2003.

[7] A.S. Daryoush and M. Ghanevati, "True time delay challenge in optically controlled phased array antennas," Digest IEEE 1997 Antennas and Propagation Society International Symposium, vol.2, pp. 732-735, 1997.

[8] K. Poulton, K. Knudsen, J. Kerley, J. Kang, J. Tani, E. Cornish, and M. VanGrou, "An 8-GSa/s 8-bit ADC system," Digest of Technical Papers in *Symposium on VLSI Circuits*, pp. 23, June 1997.

[9] K. Kitayama and B. Jalali, "Ultrafast Analog-to-Digital (A/D)Conversion Technique and its Applications," *Workshop WMK in 2007 IEEE International Microwave Symposium*, Honolulu, HI, June 2007.

[10] T. R. Clark, J. U. Kang, and R. D. Esman, "Performance of a time- and wavelength-interleaved photonic sampler for analog-digital conversion," *IEEE Photonics Technology Letter*, Volume: 11 Issue: 9 , pp.1168 –1170, 1999.

[11] A.S. Daryoush, X. Hou, W. Rosen, "All-optical ADC and its applications in future communication satellites," *Proc. IEEE 2004 Microwave Photonics Conf,* pp. 182- 185, Oct. 2004.

[12] S. Bhushan, P. V. Kelkar, B. Jalali, O. Boyraz and M. Islam, "130-Gsa/s Photonic Analog-to-Digital Converter with Time Stretch Preprocessor," *IEEE Photonic Technology Letters*, Vol. 14, No. 5, pp.684-686, 2002.

[13] A.S. Daryoush, H-W.Li, M. Kaba, G. Bouwmans, D. Decoster, J. Chazelas, and F. Deborgies, "Passively Temperature Stable Opto-electronic Oscillators Employing Photonic Crystal Fibers?" Proc. European Microwave Assoc. Vol. **3**, pp. 201–209, September 2007.

[14] D. Chen, H. R. Fetterman, A. Chen, W. H. Steier, L. R. Dalton, W. Wang, and Y. Shi, "Demonstration of 110 GHz electro-optic polymer modulators," *Appl. Phys*. Lett., vol. 70, no. 25, pp. 3335-3337, Jun. 1997.

[15] M. Oh, H. Zhang, C. Zhang, H. Erlig, Y. Chang, B. Tsap, D. Chang, A. Szep, W. H. Steier, H. R. Fetterman, and L. R. Dalton, "Recent advances in electrooptic polymer modulators incorporating highly nonlinear chromophore," *IEEE J. on Selected Topics in Quantum Electronics*, vol. 7, no. 5, pp. 826-835, Sept/Oct. 2001.

[16] V. Boucher, J. Cardin, D. Leduc, R. Seveno, R. Le Ny, H. Gundel, C. Boisrobert, S. Legoupy, F. Legros, V. Montembault, F. Odobel, E. Blart, C. Monnereau, D. Bosc, A. Goullet, J. Y. Mevellec, "Synthesis and characterization of polymers for nonlinear optical applications", *Advanced Optical Materials*, 5122, pp. 209-212 (2003).